Guidelines for EMT Transmission Line Models for Time-Domain Protection Algorithms

Joachim Vermunicht, Willem Leterme, Mudar Abedrabbo, Dirk Van Hertem
Dept. Electrical Engineering, KU Leuven/EnergyVille
Leuven/Genk, Belgium
joachim.vermunicht@esat.kuleuven.be

***Abstract*—New transmission line protection methods have been proposed for improved speed and dependability in future power systems with new elements such as VSC HVDC converters. These new methods either implicitly assume or explicitly use a transmission line model, which may vary from very simple to very detailed. The absence of a verification of these models may impact dependability and result in unwanted behaviour, especially for those algorithms that do not explicitly filter out a specific frequency (e.g., the fundamental). This paper presents a verification step in the frequency domain to assess the line model accuracy within the bandwidth of the algorithm and applies this with examples. Second, to make algorithm design choices explicit, an analysis of the line model–algorithm interactions is provided. The paper finds that the protection input filter should match the bandwidth for which the line model is accurate. A carefully designed input filter thus depends on algorithm design choices and constraints such as line geometry, line model and sample rate.**

***Index Terms*—HVDC transmission, Input filter, Protection algorithm, Time-domain protection, Transmission line modelling**

I. Introduction

New grid elements such as High Voltage Direct Current (HVDC) interconnections, converter interfaced generation and (underground) cables are being deployed in the context of renewable energy transition. This evolution results in changed characteristics of the power system during faults. At the AC side, converters have limited fault current capability (i.e. 1-1.2 p.u. compared to 8 p.u. for synchronous generators [1], [2]), and a controlled fault response causing current phase shifts depending on the control strategy [3]. Changed fault characteristics challenge currently installed protection, which becomes undependable or too slow. For example in case of a radial system ended by a converter, or a relatively large converter current contribution in a meshed system (i.e. a low grid strength), traditional distance protection malfunctions [3]–[8]. At the DC side, DC protection algorithms are needed that comply with stringent detection time requirements [9].

Time-domain protection algorithms have been developed, but not yet (widely) used, to provide for the need of fast and dependable protection e.g. [10]–[14]. These protection algorithms use different transmission line models, ranging from simple to detailed, state-of-the-art line models. The complexity of line models used in protection algorithms has increased over time, i.e. from RL models to Π, cascaded Π, and even up to the Universal Line Model (ULM) [15].

The selection of a line model for implicit or explicit application within a protection algorithm is often based on assumptions or good practices during design. These design choices however, impact important characteristics of protection algorithms e.g., sample rate, applicability for different line geometries, etc. In general, a final verification of the line model implemented in the algorithm is in most cases omitted. This means no assessment of the deviation error is made between (i) line model assumptions adopted during implementation within the algorithm and (ii) the actual transmission line behaviour.

First, this paper clarifies the interactions between line model and protection algorithm design choices. Second, this paper applies frequency domain verification to assess the deviation error introduced by line model approximations made during the design of protection algorithms. The importance of this verification step is shown with three case studies.

This work is part of the Neptune project, supported by the Energy Transition Fund, FOD Economy, Belgium.

II. Analysis of protection algorithm and transmission line model interactions

Two types of transmission line protection algorithms can be distinguished, in which the transmission line model has a central role (Fig. 1). For both algorithm types, the measurements can be passed through an input filter. The algorithm either computes fault parameters such as fault location and resistance through fitting (type *a*), or determines the presence of a fault through estimating the state based on a healthy transmission line (type *b*). The algorithm either explicitly implements a transmission line model or implies a line model through assumptions. Finally the algorithm decides whether the line is faulted or healthy.

A. Protection algorithm design

An overview of the constraints, choices and objectives considered in this paper for protection algorithm design is given in Fig. 2. Iteration on the design choices, allows to evaluate for example line model approximations with regard to accuracy and speed.

During design of the protection a trade-off is made between different objectives. Design choices (e.g. transformation to the modal domain) impact this trade-off. To reduce the algorithm's complexity and improve speed, different choices of line model and approximations are made by designers. Line models that

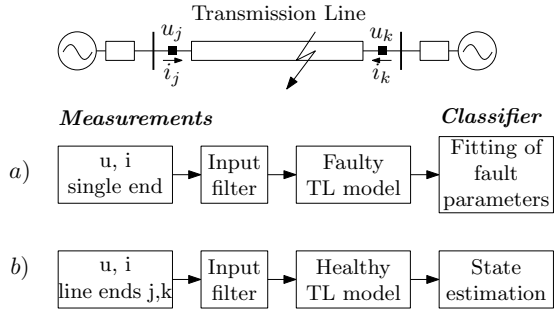

Fig. 1: The general structure for two types of transmission line (TL) protection algorithms. Type *a* needs measurement inputs from a single line end, type *b* needs inputs from both ends of the line.

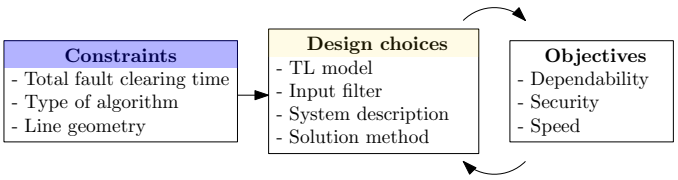

Fig. 2: Algorithm design with iterative evaluation of the design choices.

accurately simulate high-frequency transients typically require more computations than models valid for low frequencies. During design however, the accuracy of the implemented line model should be evaluated in a final verification step. This paper emphasizes the importance of validating the line model for the frequency range of interest, which is determined by the protection input filter (Fig. 1).

B. Decomposition of transmission line model–protection algorithms interactions

The diagram in Fig. 3 describes the interactions for the selection of transmission line models for protection algorithms. This approach allows to make design choices explicit. At the lower left of this diagram are theoretical aspects of line modelling such as line geometry, line model or bandwidth of interest. On the right of the diagram are solver aspects i.e. solution method and computational complexity. The system description (e.g. transfer function, state-space representation) and solution method (e.g. numerical integration or numerical inverse Laplace transform) are out of scope for this paper. The focus of this paper is on the line model for a selected bandwidth.

C. Maximum detection time

The maximum detection time - a part of the total fault clearing time - is a constraint based on stability requirements and component requirements such as maximal thermal and electromagnetic stresses exerted on system components [9]. This detection time is assumed to be known and is a constraint for both the sample rate (solution time step) of the line model and algorithm computation time (respectively arrows 1 and 4 in Fig. 3). The computation time of the algorithm should be smaller than the sampling time to allow real-time operation of the protection algorithm.

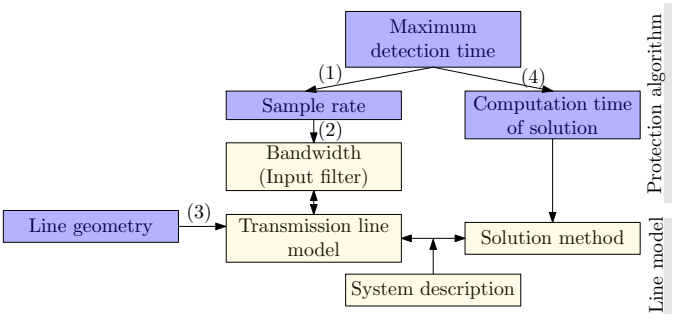

Fig. 3: Decomposition of transmission line model–algorithm interactions. Constraints are indicated in blue, design choices in yellow. This paper focuses on the line model and the interactions indicated with a number.

The line model should be carefully selected to accurately represent the transmission line within a given bandwidth (arrow 2 in Fig. 3) and for a given line geometry (arrow 3 in Fig. 3). This bandwidth depends on the solution time step of the line model and thus the sample rate of the measurements, and on the protection input filter. This input filter is for example a low pass filter (LPF), notch filter around a narrow frequency band, or high pass filter (HPF).

D. Line geometry

Geometrical characteristics of the protected line pose requirements on the type of transmission line model (arrow 3 in Fig. 3). Table I links commonly used line models with the following geometrical characteristics:

- C1: (Electrical) length of the line
- C2: Frequency dependent parameters
- C3: Multi-phase line
- C4: Asymmetry

TABLE I: Transmission line model and line geometry characteristics. "v" Means a characteristic can be included, "-" means not included.

Line model	C1	C2	C3	C4
Ideal [16]	medium-long	-	v	v
Bergeron [17]	medium-long	-	v	v
ULM [15]	medium-long	v	v	v
Single lumped section	short	-	v	v
Cascaded lumped section	short-medium	-	v	v
Rational approximations	short-long	v	v	v

C1: The line length determines the propagation delay of the line. Traveling wave, or scattering models require a minimum delay time to decouple both line ends, which determines the maximum time-step (minimum sample rate). The advised time-step is one order of magnitude smaller than delay time of the transmission line [18]. The electric length of a line (at a given frequency) is a measure for the distributed behaviour of the line, which affects the requirements for accurate modelling. For lengths smaller than a quarter wavelength, hyperbolic function correction can be omitted [16].

C2: In general, the p.u. length line parameters vary with frequency. Including the frequency dependency of line

parameters introduces additional complexity. Fitting methods such as vector fitting allow for rational approximation of the frequency dependent parameters.

C3: Multiphase transmission lines have multiple conductors, with coupling between those conductors. The mathematical formulations then consist of vectors for the voltage and current, and matrices for the impedance and admittance. The off-diagonal elements in these matrices represent the coupling terms.

C4: Asymmetric lines require a solution in the phase domain. The mathematical transformation from phase to modal domain exhibits difficulties with the decoupling of individual modes for asymmetric lines [19]. This is caused by frequency dependent transformation matrices. Line symmetry depends on the geometric configuration and other factors such as transposition or grounding (for cables).

III. Model verification methodology

Although often omitted, a verification step should quantify the approximations stemming from the design choices (section II). This verification step assesses if the line model is accurate within the bandwidth for which the protection algorithm was designed. This verification allows to evaluate the algorithm design choices and to adjust the protection input filter if needed.

A. Frequency domain verification of short circuit impedance

The proposed verification method is a frequency domain assessment. More specifically, a comparison of the line model implemented in the algorithm with a state-of-the-art benchmark line model. The benchmark line model computes frequency dependent line propagation parameters from line geometry and conductor parameters, and was validated to commercial EMT software [18]. This validation compared the short circuit impedance in the frequency domain. The short circuit impedance was constructed as in (1) from the fitting data of the propagation function and characteristic admittance from a state-of-the-art rational approximation routine.

The short circuit impedance (Z_{sc}) is the line characteristic selected for verification in the frequency domain [19], [20]. This characteristic closely relates to algorithm type *a* (Fig. 1). For algorithm type *b*, this would be the propagation function H. Z_{sc} however relates to H, e.g. for a single conductor by (1) with characteristic impedance Z_c, propagation constant γ and line length l. To obtain a general method, Z_{sc} is selected.

$$Z_{sc} = Z_c \tanh(\gamma l) = Z_c \frac{1/H - H}{1/H + H} \tag{1}$$

The relative error (ϵ) of the short circuit impedance allows to evaluate the accuracy of the line model within a specified bandwidth. For example a maximum 5% relative error threshold of the magnitude and phase at all considered frequencies [20]. Or if the behaviour at single frequencies is of less importance: a weighted error over the considered frequency range with weight function $w(f)$.

$$\epsilon = \int_0^\infty w(f) \left| \frac{Z_{sc}(f) - Z'_{sc}(f)}{Z_{sc}(f)} \right| \mathrm{d}f \tag{2}$$

B. Verification of modal domain line models implemented in algorithms

The frequency dependent transformation to the modal domain (validation in Fig. 4) allows to evaluate the approximation made with a constant transformation. In the modal domain Z_{sc} is a diagonal matrix after frequency dependent transformation. For off-diagonal elements, the deviation from zero indicates the error caused by constant transformation.

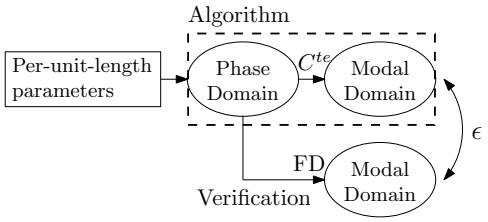

Fig. 4: Verification of a modal domain line model applying a constant (C^{te}) transformation against a frequency dependent (FD) transformation.

Protection algorithms can apply transformation to the modal domain as a design choice to simplify computational complexity. This transformation however introduces an error and should therefore be validated for its particular application. Algorithms operating in the modal domain use a constant transformation matrix e.g. in [10], [21], [22]. Often the Clark transformation is used for this purpose, because of its real and constant transformation matrix [23]. In reality however, line geometries are asymmetric and consequently the transformation matrices are frequency dependent in which case a constant transformation thus introduces an error.

IV. Results

Frequency domain verification allows to assess the approximations made during the design of protection algorithms. The importance of line model verification for models implemented in protection algorithms is shown with three case studies. For these algorithms, first the diagram of Fig. 3 is applied, then the design choices are evaluated based on the short circuit impedance and followed by a discussion. These algorithms (one of type *a* and two of type *b*) were selected for a diversity of techniques, to show that the method is generally applicable.

A. Case 1: Cascaded Π model

1) Decomposition:

The type *b* algorithm from [11] provides a sub-millisecond detection time. The frequency range of interest is 0 - 2.4 kHz with a sampling rate of 4.8 kHz. Computation time takes a fraction of the time between two consecutive samples. The implemented line model is a cascade of Π sections, with parameters evaluated at a single frequency and multi-phase configuration with asymmetry possible (full matrices). The

system description of the line is a state-space representation, using a numerical integration for the solution.

2) Discussion:

The implemented line model captures the distributed characteristic of the TL. By contrast, it neglects the frequency dependency of the line parameters. Cascading short line sections approximates the distributed character of a transmission line [19]. The cascaded Π model is accurate for a limited frequency range, 100 Hz−3 kHz in this example (Fig. 5). Outside this range, the cascaded Π model deviates from the benchmark. The line parameters of the cascaded Π model are evaluated at 1 kHz, around the first resonance peak. The ideal line model is added for comparison. The ideal line model shows less deviation at lower frequencies and captures the resonant peaks around the evaluation frequency of the line parameters. However, the ideal line model shows low damping at high frequencies

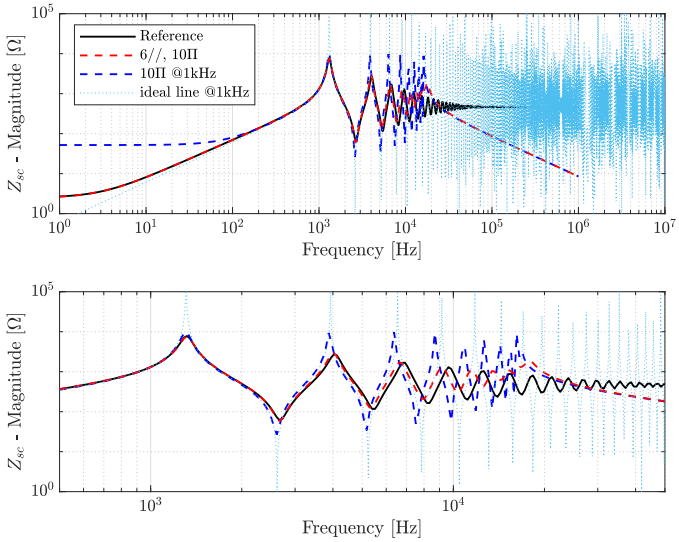

Fig. 5: Short circuit impedance of cascaded Π models and the ideal line model. The benchmark model is added as a reference. Zoom at the bottom.

Frequency variation of line parameters may be included via parallel branches in the sections of the cascaded Π model [20]. The parameters for this model are calculated with vector fitting [24]–[26]. This frequency dependent Π model is accurate for low frequencies and up to higher frequencies than the conventional cascaded Π model. For example, the frequency dependent Π model with 6 parallel branches and 10 sections is close to the benchmark in the range 1 Hz−6 kHz (Fig. 5). However, a frequency dependent, cascaded, 3-phase Π model which includes coupling between the phases does not yet exist.

Decomposition into modes or symmetrical components could provide separate (sequence) networks with either approximately constant or frequency dependent line parameters, but this does not resolve coupling between phases. For the aerial mode, increasing the number of conventional cascaded Π sections results in better fitting of the aerial mode up to higher frequencies (Fig. 6). The aerial mode for overhead lines exhibits low frequency dependency at high frequencies [27]. For the ground return mode, the same is not true (Fig. 6). The majority of faults however is phase-to-ground and includes the ground mode.

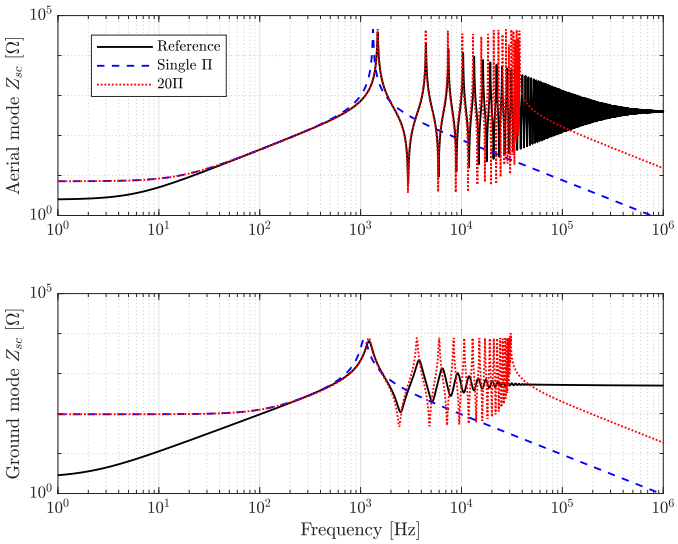

Fig. 6: Short circuit impedance of the aerial and ground return modes for a 2 conductor TL, with line parameters evaluated at 1 kHz.

Cascaded models present spurious high frequency oscillations when applying step functions in the time domain [28]. This is caused by reflections at the junctions of individual line sections [16]. Moreover, the deviation error of the magnitude of Z_{sc} is significant at high frequencies and increases linearly with the frequency on log scale (see Fig. 5). As a result, low pass filtering is needed for the protection algorithm.

3) Conclusion:

The protection algorithm requires a carefully designed input filter which matches the bandwidth of the line model. The cascaded Π model is compared to the benchmark line model (Fig. 5). Verification shows that this line model is accurate for a limited bandwidth around the evaluation frequency of the p.u. length parameters. Oscillations caused by resonances, that are not filtered by a protection input filter (with matching bandwidth), potentially affect the accuracy of the algorithm.

B. Case 2: Aerial and ground mode for the ideal line model

1) Decomposition:

The type *a* algorithm in [10] aims at a detection time of 0.5 ms. The frequency range of interest is 167 kHz – 0.5 MHz (1 MHz sampling rate). The implemented line model is an ideal line model (lossless and with constant line parameters) for aerial and ground modes, with a separate behavioral first order model to include ground effects. The system description of the line model is a transfer function for the first n traveling wave reflections. The selected solution method is numerical integration.

2) Discussion:

Transformation to the modal domain into aerial and ground modes is done using a constant transformation matrix (containing eigenvectors at a single frequency). In reality, line geometries are asymmetric and consequently the

transformation matrices are frequency dependent. A constant transformation thus introduces an error.

Two line geometries are considered to compare the off-diagonal elements (section III): an asymmetric and near-symmetric geometry. The asymmetric geometry consists of 3 conductors (phases) arranged vertically above the ground. The near-symmetric geometry consists of 3 conductors arranged horizontally above the ground at equal distance. In the latter case the 3 phase conductors have similar euclidean distance to the ground. To show the effects of line geometry in modal transformation, the comparison in this paper uses the benchmark model as a reference. By contrast, algorithm [10] applies the ideal line model. The ideal line model includes the delay effect of distributed lines (resonant peaks), but shows low damping at high frequencies (Fig. 5).

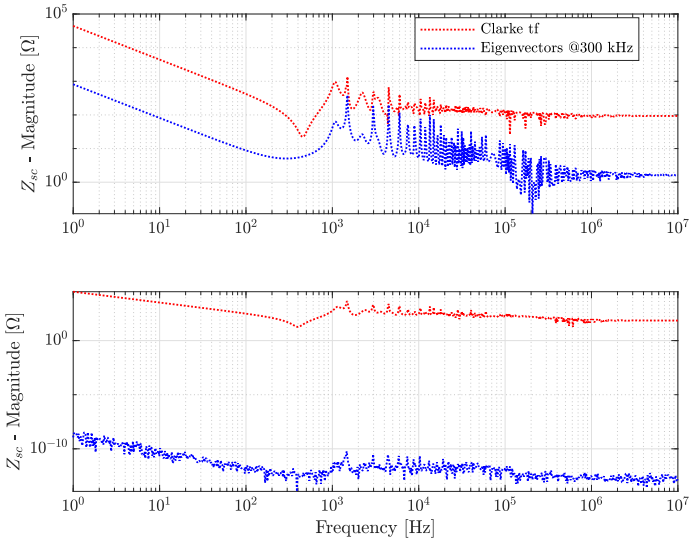

Fig. 7: Short circuit impedance of off-diagonal element (1,2) in the modal domain. For an asymmetric geometry at the top and near-symmetric geometry at the bottom. In red: Clarke transformation; in blue: transformation matrix evaluated at a single frequency. The reference with frequency dependent transformation is zero.

For the near-symmetric geometry, the off-diagonal elements are close to zero for a constant transformation matrix based on eigenvectors (blue curve in Fig. 7). Furthermore, the frequency variation of the eigenvectors is limited. The diagonal elements of the frequency dependent benchmark model match those of the constant transformation matrix based on eigenvectors (Z_{sc}(1,1) in Fig. 8). By contrast, for the asymmetric geometry, the off-diagonal elements are non-negligible. Applying the Clarke transform results in off-diagonal elements with non-negligible magnitude for both line geometries (red curves in Fig. 7) and introduces an error in the diagonal elements at high frequencies. For the benchmark model which applies frequency dependent transformation matrices, all off-diagonal elements are zero as expected.

3) Conclusion:

For near-symmetric lines, the modal transformation is a reasonable and useful design choice to decrease the algorithm's computational complexity. Verification is done for two example line geometries and it is shown that

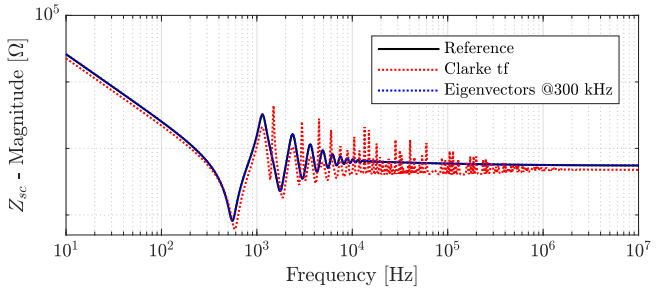

Fig. 8: Short circuit impedance of diagonal element (1,1) in the modal domain, for the near-symmetric geometry. In black: frequency dependent transformation; in red: Clarke transformation; in blue: transformation matrix evaluated at a single frequency.

transformation to the modal domain with a constant transformation matrix can introduce a significant error. The assumption of constant matrices thus requires verification taking into account the line geometry (section II-D) across the considered bandwidth, which is determined by the protection input filter.

The protection input filter (e.g. for algorithm [10]) therefore should be carefully designed to match the bandwidth of the selected line model, which needs validation to a benchmark model. For this algorithm, the maximum frequency and sampling rate should be sufficiently high to capture traveling waves originating from a fault close to the bus (minimal line length) [19]. The lower frequency limit is determined by taking into account the first n reflections during a small time window for fitting of the fault parameters.

C. Case 3: Universal line model

1) Decomposition:

The type *b* algorithm from [12] has an unspecified detection time. The requirement for DC protection is in the millisecond range [9]. The frequency range of interest is DC (0 Hz) to a high, unspecified, maximum frequency. Computation time is not mentioned. The implemented line model is the Universal Line Model, with frequency dependent line parameters. The system description of the line model is the impulse response, derived from the transfer function. The time-domain solution is computed via rational fitting and recursive convolution.

2) Discussion:

The algorithm implements a state-of-the-art line model with a phase domain solution. Verification in the modal domain (Fig. 4) is thus not applicable. The main approximations are DC correction in the rational fitting of the frequency dependent propagation function and approximation of the propagation delay. Verification requires a benchmark transmission line model that does not make these approximations, e.g. the analytic Π section with hyperbolic correction functions [16]. These approximations are not in the scope of this paper. Further details and improvements on low frequency behaviour can be found e.g. in [29]. The model in [12] uses a similar approach to compute the line propagation parameters as the benchmark model in this paper. Therefore, trivial verification results are not provided.

3) Conclusion:

Verification in the modal domain is not applicable for line models with a direct phase domain solution. Instead, frequency domain verification can be done in the phase domain. The method (section III) remains similar in general: a verification step in the frequency domain over a specified bandwidth, to evaluate algorithm design choices and to adjust the protection input filter accordingly.

V. Conclusion

Frequency domain verification allows to evaluate transmission line model accuracy with respect to the trade-off in protection algorithm objectives. Different trade-offs are made in algorithm design that significantly impact line model accuracy, for example to reduce the algorithm's complexity and improve speed. However, verification of the line model implemented in the algorithm is often missing. The bandwidth for which a line model is accurate often not corresponds with the bandwidth of the protection input filter, or this input filter is omitted. The bandwidth of a carefully designed input filter depends on algorithm design choices and constraints such as line geometry, line model and sample rate.

Based on examples, this paper explicates protection algorithm limitations in a generic manner. The verification method first computes the short circuit impedance of both the line model implicitly assumed or explicitly used by the protection algorithm, and a benchmark transmission line model as function of frequency. Then, the deviation between both models is evaluated within the bandwidth determined by the protection input filter. This approach allows to assess approximations made during algorithm design. Additionally, conditions of application can be identified e.g., application for a specific line geometry or a restricted protection input filter bandwidth.

Bibliography

[1] R. Wachal et al., "Guide for the development of models for HVDC converters in a HVDC grid," in *Cigré working group B4.57*, 2014.

[2] J. A. Martinez-Velasco, *Power system transients: parameter determination*. CRC press, 2017.

[3] A. Hooshyar, M. A. Azzouz, and E. F. El-Saadany, "Distance Protection of Lines Emanating From Full-Scale Converter-Interfaced Renewable Energy Power Plants—Part I: Problem Statement," *IEEE Transactions on Power Delivery*, vol. 30, pp. 1770–1780, Aug. 2015.

[4] C. Brantl, P. Ruffing, and R. Puffer, "The application of line protection relays in high voltage ac transmission grids considering the capabilities and limitations of connected mmcs," in *15th International Conference on Developments in Power System Protection (DPSP 2020)*, (Liverpool, UK), pp. 1–6, 2020.

[5] M. M. Alam, H. Leite, J. Liang, and A. da Silva Carvalho, "Effects of vsc based hvdc system on distance protection of transmission lines," *International Journal of Electrical Power & Energy Systems*, vol. 92, pp. 245–260, 2017.

[6] J. Jia, G. Yang, A. H. Nielsen, and P. Roenne-Hansen, "Hardware-in-the-loop tests on distance protection considering vsc fault-ride-through control strategies," *The Journal of Engineering*, vol. 2018, no. 15, pp. 824–829, 2018.

[7] J. J. Chavez, M. Popov, A. Novikov, S. Azizi, and V. Terzija, "Protection function assessment of present relays for wind generator applications," in *International Conf. on Power Systems Transients (IPST2019)*, (Perpignan, France), pp. 1–6, 2019.

[8] A. Haddadi, M. Zhao, I. Kocar, U. Karaagac, K. W. Chan, and E. Farantatos, "Impact of inverter-based resources on negative sequence quantities-based protection elements," *IEEE Transactions on Power Delivery*, vol. 36, no. 1, pp. 289–298, 2021.

[9] W. Leterme and D. Van Hertem, "Classification of fault clearing strategies for hvdc grids," in *CIGRE, Date: 2015/05/27-2015/05/28, Location: Lund*, 2015.

[10] P. Verrax, A. Bertinato, M. Kieffer, and B. Raison, "Fast fault identification in bipolar hvdc grids: A fault parameter estimation approach," *IEEE Transactions on Power Delivery*, vol. 37, no. 1, pp. 258–267, 2022.

[11] A. P. S. Meliopoulos, G. J. Cokkinides, P. Myrda, Y. Liu, R. Fan, L. Sun, R. Huang, and Z. Tan, "Dynamic State Estimation-Based Protection: Status and Promise," *IEEE Transactions on Power Delivery*, vol. 32, pp. 320–330, Feb. 2017.

[12] N. Johannesson and S. Norrga, "Longitudinal differential protection based on the universal line model," in *IECON 2015 - 41st Annual Conference of the IEEE Industrial Electronics Society*, (Yokohama, Japan), pp. 1091–1096, 2015.

[13] N. Hoxha, *Ultra-fast line protection relay algorithm based on a Gamma model of line*. PhD thesis, Université libre de Bruxelles, Ecole polytechnique de Bruxelles, Bruxelles, 2020.

[14] Schweitzer Engineering Laboratories, *SEL-T400L Ultra-High-Speed Transmission Line Relay Traveling-Wave Fault Locator High-Resolution Event Recorder Instruction Manual*. Schweitzer Engineering Laboratories, 20190430.

[15] A. Morched, B. Gustavsen, and M. Tartibi, "A universal model for accurate calculation of electromagnetic transients on overhead lines and underground cables," *IEEE Transactions on Power Delivery*, vol. 14, no. 3, pp. 1032–1038, 1999.

[16] J. Marti, L. Marti, and H. Dommel, "Transmission line models for steady-state and transients analysis," in *Proceedings. Joint International Power Conference Athens Power Tech,*, vol. 2, pp. 744–750, Sept. 1993.

[17] H. W. Dommel, "Digital computer solution of electromagnetic transients in single-and multiphase networks," *IEEE Transactions on Power Apparatus and Systems*, vol. PAS-88, no. 4, pp. 388–399, 1969.

[18] Manitoba HVDC research centre, *User's Guide, on the use of PSCAD*. Manitoba, Canada, 2018.

[19] S. Grivet-Talocia and B. Gustavsen, *Passive macromodeling: Theory and applications*. John Wiley & Sons, 2015.

[20] S. D'Arco, J. A. Suul, and J. Beerten, "Analysis of accuracy versus model order for frequency-dependent pi-model of HVDC cables," in *2016 IEEE 17th Workshop on Control and Modeling for Power Electronics (COMPEL)*, pp. 1–8, 2016.

[21] M. M. Mansour and G. W. Swift, "A multi-microprocessor based travelling wave relay - theory and realization," *IEEE Transactions on Power Delivery*, vol. 1, no. 1, pp. 272–279, 1986.

[22] M. Bollen, *On travelling-wave-based protection of high voltage networks*. PhD thesis, TU Eindhoven, Eindhoven, The Netherlands, 1989.

[23] M. Tavares, J. Pissolato, and C. Portela, "Mode domain multiphase transmission line model-use in transient studies," *IEEE Transactions on Power Delivery*, vol. 14, pp. 1533–1544, Oct. 1999.

[24] B. Gustavsen and A. Semlyen, "Rational approximation of frequency domain responses by vector fitting," *IEEE Transactions on power delivery*, vol. 14, no. 3, pp. 1052–1061, 1999.

[25] B. Gustavsen, "Improving the pole relocating properties of vector fitting," *IEEE Transactions on Power Delivery*, vol. 21, no. 3, pp. 1587–1592, 2006.

[26] D. Deschrijver, M. Mrozowski, T. Dhaene, and D. De Zutter, "Macromodeling of multiport systems using a fast implementation of the vector fitting method," *IEEE Microwave and wireless components letters*, vol. 18, no. 6, pp. 383–385, 2008.

[27] W. Leterme, S. P. Azad, and D. Van Hertem, "HVDC grid protection algorithm design in phase and modal domains," *IET Renewable Power Generation*, vol. 12, no. 13, pp. 1538–1546, 2018.

[28] A. R. J. Araújo, R. C. Silva, and S. Kurokawa, "Comparing lumped and distributed parameters models in transmission lines during transient conditions," in *2014 IEEE PES T&D Conference and Exposition*, pp. 1–5, 2014.

[29] M. Cervantes, I. Kocar, J. Mahseredjian, and A. Ramirez, "Partitioned fitting and dc correction for the simulation of electromagnetic transients in transmission lines/cables," *IEEE Transactions on Power Delivery*, vol. 33, no. 6, pp. 3246–3248, 2018.